

QUADRUPOLE TRANSITION SPECTRUM MEASUREMENT OF SINGLE Ca⁺ IONS TOWARD OPTICAL FREQUENCY STANDARDS

**Kensuke Matsubara, Ying Li, Kyoya Fukuda, Hiroyuki Ito,
Shigeo Nagano, Masatoshi Kajita, Kazuhiro Hayasaka, Shinji Urabe*,
and Mizuhiko Hosokawa**

National Institute of Information and Communications Technology

***Graduate School of Engineering Science, Osaka University**

4-2-1 Nukui-Kitamachi, Koganei, Tokyo 184-8795, Japan

E-mail: *matubara@nict.go.jp*

Abstract

The National Institute of Information and Communications Technology in Japan is proceeding with development of an optical frequency standard using an electric quadrupole transition of Ca⁺ ions in a small radio-frequency trap. The single, trapped ⁴⁰Ca⁺ ions are laser-cooled to a temperature of <10 mK using extended-cavity diode lasers at 397 nm and 866 nm. In order to measure the electric quadrupole transition, the linewidth of the clock laser diode at 729 nm is reduced to ~66 Hz using an ultra-low-expansion (ULE) cavity. We observed the electric quadrupole transition with a linewidth of ~600 kHz, together with the ionic motional sidebands. We are also developing optical frequency combs without photonic fibers broadening the spectrum. The experimental is now improved in order to observe the narrower linewidth of the quadrupole transition.

I. INTRODUCTION

The uncertainty of primary frequency standards using Cs atoms reaches around 10⁻¹⁵ and their inherent limits are being discussed. Alternatively, frequency standards using new atomic and ionic materials are proposed for developing more stable and accurate frequency standards. Several groups have measured frequencies of the ionic forbidden transitions in the optical region to apply them to the clock transitions in frequency standards [1]. We now proceed with a study on an optical frequency standard using single Ca⁺ ions. One of advantages using Ca⁺ ions is that all the useful transitions are accessible with the existing laser diodes (LDs) and we can develop a compact and reliable frequency standard [2].

Partial term diagrams of ⁴⁰Ca⁺ and ⁴³Ca⁺ ions are shown in Figure 1. These ions are laser-cooled with the ²S_{1/2} – ²P_{1/2} cooling transition at 397 nm and the ²P_{1/2} – ²D_{3/2} repumping transition at 866 nm. The lifetime of the ²D_{5/2} state is ~1.2 s (natural linewidth ~0.2 Hz), which gives a very high line-Q (~10¹⁵) to the electric quadrupole ²S_{1/2} – ²D_{5/2} transition at 729 nm. An odd isotope like ⁴³Ca⁺ ions has the merit that it can avoid the first-order Zeeman frequency shift. We theoretically confirmed that an uncertainty of <1 x 10⁻¹⁵ is attainable in measurement of ⁴³Ca⁺ ions [3]. However, the laser cooling of ⁴³Ca⁺ ions

requires a much more complicated light source than that of $^{40}\text{Ca}^+$ ions because of the hyperfine splitting and their small natural abundance (0.14 %). In the case of even isotopes like the $^{40}\text{Ca}^+$ ion, the largest source of the frequency uncertainty is the first-order Zeeman shift. However, a new way to reduce this uncertainty was illustrated [4]. According to the measurement of $^{88}\text{Sr}^+$ ions [5], whose total uncertainty was 3.4×10^{-15} , it would be possible to reduce the uncertainty of a $^{40}\text{Ca}^+$ ion due to the first-order Zeeman shift on the order of 10^{-15} . Therefore, we now aim to measure the $^2S_{1/2} - ^2D_{5/2}$ transition of $^{40}\text{Ca}^+$ ions with high accuracy using a simple laser-cooling light source system. In Section II, we explain the development of the light sources required for $^{40}\text{Ca}^+$ ions, and spectroscopy follows in Section III. The development of optical frequency combs used for accurate measurement of the clock transition frequency is shown in Section IV. Finally, the concluding remarks and the future plan are described.

II. LIGHT SOURCES

In order to measure the electric quadrupole $^2S_{1/2} - ^2D_{5/2}$ transition of $^{40}\text{Ca}^+$ ions, we developed coherent light sources at 397 nm, 866 nm, 729 nm, 429 nm, 374 nm, and 854 nm based on laser diodes. All the light sources except for one at 854 nm are shown in the following subsections. The 854-nm one is a Littman-type extended-cavity diode laser (ECDL) frequency-stabilized with a confocal optical resonant cavity, which is used to repump the ion from the $^2D_{5/2}$ state to the laser cooling cycle after absorbing the photon of the clock laser.

A. COOLING LASERS

For the laser cooling of $^{40}\text{Ca}^+$ ions, we developed a light source system shown in Figure 2. It consists of an 866-nm part, a 397-nm part, a frequency-stabilized He-Ne laser, and a function generator. Details of this light source system are reported in [6]. The Littrow-type ECDLs at 866 nm (Toptica) and 397 nm (Nichia) are used as the slave laser [7], while the He-Ne laser is the master laser. In the 866 nm part, both the laser beams from the ECDL and the He-Ne laser are coupled to a single scanning transfer cavity.

The cavity is placed in an airtight container made of an aluminum tube and AR-coated windows. Temperature variance around the container is kept to within ± 0.1 K. Triangular waves of the function generator govern the cavity-length scanning. Its rate is 1 kHz and the scanning width is $5/3$ FSRs (500 MHz) for the He-Ne laser (633 nm). The both transmission powers at photo-diodes (PDs) are fed to a personal computer (PC) through a high-speed analog-digital converter. In the first half of each triangular-wave cycle, the PC sampled the PD signals at a sampling frequency of 4 MHz. The number of the sampled signals between the two consecutive transmission peaks of the He-Ne laser, denoted by A here, is counted. The number of signals between one peak of the master laser and that of the 866-nm laser, denoted by B , is also counted. For every cavity scan, the ratio $\alpha = B/A$ is compared to a constant α_0 determined by the first cavity scan, and the 866-nm frequency is calibrated so as to make α closer to α_0 .

The scanning region of the transfer cavity is fixed by keeping the number of signals between the first master-laser peak and a trigger signal synchronized to the triangular waves constant. The 397 nm LD is stabilized in the same manner.

Frequency stability of the 866-nm light was measured by an optical frequency comb (FC8003, Menlo Systems) [8]. In Figure 3, it is shown that the stability is improved ~ 100 times better by this method. The frequency drift was ~ 300 kHz for 2 h for the stabilized ECDL. The short-term end of Figure 3 implies that this method can improve the stability in the term shorter than 1 s. Although the stability of the 397-nm ECDL could not be measured using our frequency synthesizer, it was estimated that the frequency drift at 397 nm was smaller than 2 MHz per hour considering dispersion of the refractive index that depends on wavelength and the air condition. These stabilities are enough for the laser cooling of

Ca⁺ ions because the drifts are much smaller than natural widths of the cooling and the repumping transitions.

B. CLOCK LASER

To measure the $^2S_{1/2} - ^2D_{5/2}$ quadrupole transition of Ca⁺ ions, we developed a highly stable frequency-tunable master-and-slave laser-diode source at 729 nm. In Figure 4, the experimental setup is shown, and its explanation is given in [9]. For the master laser, an AR-coated LD (Toptica) is used in an ECDL with the Littman configuration. To compress its linewidth and frequency drift, the output of the master ECDL is coupled to a high-finesse ($F = 6 \times 10^4$), 1-GHz-FSR ultra-low-expansion (ULE) optical cavity after it passes through an electro-optic modulator (New focus) generating weak FM sidebands at 15 MHz and a polarization-maintaining (PM) single-mode fiber producing a single spatial mode. The ULE cavity is put in a chamber evacuated to a pressure of 10^{-6} Pa and the chamber temperature was stabilized to within ± 0.01 K. The chamber is mounted on a vibration-canceling platform, and the whole the system is placed in an acoustic isolation box. A Si photodiode (Hamamatsu) monitors the reflected light from an ULE-cavity mirror. The signal is demodulated [10], integrated, and fed back to the master ECDL using both a fast current feedback loop and a relatively slow PZT feedback loop, so that the ECDL frequency is stabilized. For evaluation of the linewidth of the master laser, we measured the heterodyne beatnote frequency between two master lasers using the identical stabilization method, where each of them is locked to an individual ULE cavity. It is shown in Figure 5. The data acquisition time is 3 s and the measurement resolution is 1 Hz. We estimated the full width at half maximum (FWHM) of the master laser linewidth to be 66 Hz from the measured beatnote linewidth.

In order to measure the transition spectrum, frequency tunability is indispensable for the light source system. For this purpose, we measured the beatnote between a slave ECDL and the master one using a fast PD. The phase difference between the beatnote and an output of a reference local oscillator, which is linked to a hydrogen maser, is demodulated and processed in a phase-lock loop to lock the slave ECDL frequency to the master one with an arbitrary frequency difference [11]. We achieve a frequency difference range wider than 1 GHz, which covers the whole FSR of the ULE cavity. The Allan variance of the master and the slave ECDLs is measured with the commercially available optical frequency synthesizer (FC8003) linked to the International Atomic Time (TAI). The stabilities of the master and the slave ECDLs were identical, and the frequency drift was 1 ~ 2 Hz per 1 s. Since the long-term stability is now limited by the thermal stability of the ULE cavity, we are improving the temperature control system.

C. PHOTO-IONIZING LASER

It has been a conventional method that ions loaded into the ion trap are created by the electron impact to the neutral atoms. In this method, however, residual atoms patched on the trap and electrons charging the trap often degrade the trap potential so as to cause large motion of the trapped ion. Therefore, photo ionization was proposed to create the ions from very dilute atomic gases without electric charging [12]. Selective ionization of a rare isotope can be performed with this method. We developed a light source system for photo-ionization of $^{40}\text{Ca}^+$ ions based on laser diodes.

Neutral Ca atoms are ionized by a two-step photo-excitation with photons at 423 nm and at <390 nm, where the $^1S_0 - ^1P_1$ transition is accessible with the photons at 423 nm and the atoms populating the 1P_1 state is ionized with the photons at <390 nm. The 423-nm light is produced by the second-harmonic generation from 846-nm light using a periodically poled (pp) KTP crystal [13]. The 846-nm light power of about 5 mW from a Littman-type master ECDL is amplified to be ~ 60 mW by light injection to a high-

power 846-nm LD. Temperature of the pp-KTP crystal is controlled to ~ 295 K, and the 846-nm light is passed through the crystal with the single-pass configuration. We generate 423 nm light of ~ 100 μ W. It is coupled to a single-mode optical fiber, and the power of ~ 30 μ W is applied to the $^1S_0 - ^1P_1$ excitation. The light at < 390 nm is produced from a ultraviolet LD at 375 nm. We used the 374-nm light of ~ 1 mW for ionization. The frequency of 423-nm light is tuned to the $^1S_0 - ^1P_1$ transition by monitoring fluorescence from a neutral Ca beam passing through the ion trap. We experimentally confirmed that Ca atoms are ionized using this laser system.

III. SPECTROSCOPY

A. SINGLE $^{40}\text{Ca}^+$ ION TRAP AND MICROMOTION COMPENSATION

We are performing a spectroscopic study on $^{40}\text{Ca}^+$ ions, aiming to confine a single ion to a region much smaller than wavelength of 729-nm light to eliminate the first-order Doppler broadening from the $^2S_{1/2} - ^2D_{5/2}$ clock transition [14]. The experimental setup is shown in Figure 6. A small radio-frequency trap consisting of one ring electrode and two end-cap electrodes is employed for trapping a single $^{40}\text{Ca}^+$ ion. The ring electrode is made of a 0.7-mm-thick 304-stainless-steel plate, which has a 0.5-mm-radius hole. The inside wall of the hole is shaped into a semicircular cross section. The end-cap electrodes are 1.0-mm-diameter rods, whose ends are shaped to be semi-spherical. A pair of auxiliary rod electrodes is placed near the end caps to compensate the stray electric field in the trap. An rf voltage of 300 V at 19 MHz is applied to the ring electrode to produce the ion trap potential. The ion trap is put in a stainless-steel chamber evacuated to a pressure below 5×10^{-8} Pa.

At first, frequencies of the 397-nm and the 866-nm ECDLs were tuned to the resonance centers of $^{40}\text{Ca}^+$ ions using the optogalvano signals as the reference. Then, the frequency of the 397-nm one was set to ~ 100 MHz below the resonance center. After turning on the Ca oven and the photo-ionizing lasers for ~ 40 s, we scanned the frequency of the 397-nm ECDL around the resonance of the $^{40}\text{Ca}^+$ ion, and we observed the spectrum of the laser-cooled $^{40}\text{Ca}^+$ ions. The maximum photon counting rate per one $^{40}\text{Ca}^+$ ion was estimated to be ~ 7000 /s. When we observe a photon counting rate much larger than 7000/s, multiple ions should be trapped. To make number of the ion single, we fixed the 397-nm frequency on the higher frequency side of the resonance for a few tens of seconds. By this procedure, the fluorescence intensity in the laser cooling often decreased because the laser heating could make some ions drop out from the ion trap. When we confirmed a single $^{40}\text{Ca}^+$ ion trap, we proceeded to the micromotion compensation to cancel the electric stray field causing large ionic oscillation (micromotion) [15]. We measured the time correlation between the arrival of photons at the PTM and the phase of the radio-frequency field using a time-interval counter. When a large amplitude modulation is observed in the distribution of the measured interval times, a large ionic micromotion is generated. In such case, DC voltages applied to the compensation electrodes and end-cap electrodes are tuned to minimize the modulation amplitude. A typical spectrum of the laser-cooled single $^{40}\text{Ca}^+$ ion is shown in Figure 7. We measured the linewidth at various 397-nm light powers to estimate the residual Doppler width. Temperature of the $^{40}\text{Ca}^+$ ions is estimated to be < 10 mK.

B. QUANTUM JUMPS AND MOTIONAL-SIDEBAND RESOLVED SPECTRUM

When the laser-cooling spectrum as shown in Figure 7 was observed, we fixed the frequency of the 397-nm light at several MHz below the resonance and observed continuous fluorescence intensity from the single $^{40}\text{Ca}^+$ ion. The light from the slave 729-nm ECDL is superposed with the cooling lasers at 397 nm and 866 nm using a dielectric mirror. The 729-nm light was focused into the trap chamber with a beam waist of somewhat larger than those of the cooling lasers. While the 729-nm light was applied to a single $^{40}\text{Ca}^+$

ion, we observed the quantum jumps accompanied with the $^2S_{1/2} - ^2D_{5/2}$ transition. Typical measurement of the quantum jumps is shown in Figure 8. The gate time of the photon counting is set to 100 ms. When the single $^{40}\text{Ca}^+$ ion is pumped into the metastable $^2D_{5/2}$ state by absorbing the 729-nm light, fluorescence with the $^2S_{1/2} - ^2P_{1/2}$ transition is fully extinguished. The fluorescence intensity with the laser cooling returns after the ion decays back to the $^2S_{1/2}$ state from the $^2D_{5/2}$ state.

In order to observe the spectrum line profile of the $^2S_{1/2} - ^2D_{5/2}$ quadrupole transition, we measured the rate of the quantum jumps of a single $^{40}\text{Ca}^+$ ion depending on the 729-nm light frequency. The frequency of the 729-nm laser is stepped by 200 kHz and its intensity was fixed to $\sim 30 \mu\text{W}$ through the measurement. In order to eliminate the power broadening caused by the cooling laser, the 397-nm light and the 729-nm one were irradiated to the ion alternatively with the interval time of 25 ms. In addition, the 854-nm light was applied for 50 ms with intervals of 950 ms. When the 854-nm light is absorbed by the ion populating the $^2D_{5/2}$ state, the ion returns to the laser cooling cycle. The transition probability was calculated from the number of the quantum jumps that happened in one minute at each clock laser frequency. We measured the spectrum in an external magnetic field of $\sim 5 \times 10^{-4} \text{ T}$ ($\sim 5 \text{ G}$). In Figure 9, one Zeeman component is shown as a function of the 729-nm frequency detuning. In this spectrum we observed the carrier transition line and the motional sidebands with a radial secular motion of $\sim 1.6 \text{ MHz}$. Some similar profiles were measured with the linewidth of the order of 600 kHz. This width seems to have suffered from the residual Doppler broadening and the power broadening caused by the 729-nm radiation.

III. OPTICAL FREQUENCY COMB

The output of the mode-lock pulse laser can be described as a frequency comb in the frequency domain.

The frequency of the n th mode is expressed as $f_n = nf_{\text{rep}} + f_{\text{ceo}}$, where f_{rep} is the repetition frequency and f_{ceo} is the carrier-envelope offset frequency [16]. We are now developing two optical frequency combs based on different femtosecond mode-locked Ti:sapphire lasers (Venteon OS and Gigajet 20W) [17]. Because f_{ceo} can be locked in both combs without broadening the spectrum in the photonic crystal fiber, we expect a better performance than that with the photonic crystal fiber [18].

Venteon OS generates a frequency comb for more than a 1-octave wavelength span with the repetition frequency of $f_{\text{rep}} = 200 \text{ MHz}$, and f_{ceo} is locked using the self-referencing method. The experimental setup is shown in Figure 10. All the optics are fixed on a single, temperature-controlled breadboard. The frequency modes near 570 nm (f_1) and 1140 nm (f_2) are used to monitor the carrier-envelope offset frequency $f_{\text{ceo}} = 2f_2 - f_1$. This is phase-locked by feeding the error signal from the digital phase detector to the AOM that controls the pumping power. By this method, fluctuation of f_{ceo} is reduced to $< 1 \text{ mHz}$ for the measuring time of 1 s. The repetition frequency f_{rep} is monitored by using a fast PD. It is phase-locked to an output of a local oscillator linked to the hydrogen maser. The control signal produced from a double balanced mixer is fed back to slow and fast PZTs that control the cavity length. On the other hand, Gigajet 20W generates a frequency comb for less than one-octave span with $f_{\text{rep}} = 1 \text{ GHz}$. Its high repetition frequency and a high output power of 800 mW gives us the benefit of a large signal-to-noise ratio in the frequency measurement. In this system, f_{ceo} is monitored from the beatnotes between the second harmonics of the frequency modes near 640 nm (f_1') and the third harmonics of the mode near 960 nm (f_2'): $f_{\text{ceo}} = 3f_2' - 2f_1'$. The phase-locking technique for f_{rep} and f_{ceo} , is similar to that used in the Venteon OS system.

We measured the beatnote between the 729-nm clock laser and the output of each optical frequency comb, where we used two frequency combs mentioned above and a commercially available one (FC8003). The measurements were performed individually in different days. The Allan deviation of

the beatnote is shown in Figure 11. These measurements show that the frequency stability of $\sim 2 \times 10^{-13}$ in the root Allan deviation at an averaging time of 1 s. The measurement precision in the short term is presently limited by the stability of the hydrogen maser. The long-term frequency drifts are 1 ~ 2 Hz per 1 s, which is governed by the thermal stability of the ULE resonance cavity. We are now improving the temperature control of the ULE cavity.

IV. CONCLUSION

The calcium ion is very attractive for application in optical frequency standards because its $4^2S_{1/2} - 3^2D_{5/2}$ transition, whose natural linewidth is ~ 0.2 Hz, is measurable with existing LDs. By using LD-based light sources and a small ion trap, we can develop a robust and compact optical frequency standard.

For the laser cooling of Ca^+ ions, we developed a simple method stabilizing frequencies of multiple ECDLs down to the order of 100 kHz using a He-Ne laser and scanning transfer cavities. As a light source for measuring the $4^2S_{1/2} - 3^2D_{5/2}$ clock transition with a narrow linewidth, a highly stable frequency-tunable LD system at 729 nm was developed. Its linewidth was estimated to be 66 Hz. We measured a spectrum of the $4^2S_{1/2} - 3^2D_{5/2}$ transition from the rate of the quantum jump of a single $^{40}\text{Ca}^+$ ion. In this measurement, the observed spectrum was limited by the residual Doppler broadening and the power broadening by the 729-nm light. For the optical frequency measurement, we are developing two femtosecond optical frequency combs based on two different mode-lock Ti:sapphire lasers, in which f_{ceo} is locked without broadening the spectrum in photonic crystal fibers. We are improving the system towards the development of an optical frequency standard using Ca^+ ions.

REFERENCES

- [1] R. Gill, 2005, "Optical frequency standards," **Metrologia**, **42**, S125-S137.
- [2] M. Kajita, K. Matsubara, Y. Li, K. Hayasaka, and M. Hosokawa, 2004, "Preparing single ions in $m = 0$ states in the Lamb-Dicke regime," **Japan. Journal of Applied Physics**, **43**, 3592-3595.
- [3] M. Kajita, Y. Li, K. Matsubara, K. Hayasaka, and M. Hosokawa, 2005, "Prospect of optical frequency standard based on a $^{43}\text{Ca}^+$ ion," **Physical Review A** **72**, 043404.
- [4] J. E. Bernard, L. Marmet, and A. A. Madej, 1998, "A laser frequency lock referenced to a single trapped ion," **Optical Communications**, **150**, 170-174.
- [5] H. S. Margolis, G. P. Barwood, G. Huang, H. A. Klein, S. N. Lea, K. Szymaniec, and P. Gill, 2004, "Hertz-level measurement of the optical clock frequency in a single $^{88}\text{Sr}^+$ ion," **Science**, **306**, 1355-1358.
- [6] K. Matsubara, S. Uetake, H. Ito, Y. Li, K. Hayasaka, and M. Hosokawa, 2005, "Precise frequency-drift measurement of extended-cavity diode laser stabilized with scanning transfer cavity," **Japan. Journal of Applied Physics**, **44**, 229-230.
- [7] K. Hayasaka, 2002, "Frequency stabilization of an extended-cavity violet diode laser by resonant optical feedback," **Optical Communications**, **206**, 401-409.

- [8] R. Holzwarth, M. Zimmermann, T. Udem, and T. W. Hansch, 2001, “*Optical clockworks and the measurement of laser frequencies with a mode-locked frequency comb*,” **IEEE Journal of Quantum Electronics**, **37**, 1493-1501.
- [9] Y. Li, H. Ito, K. Matsubara, M. Kajita, and M. Hosokawa, 2006, “*A clock laser for the optical frequency standard of Ca^+ ion*,” in Book of Abstracts of the 20th International Conference on Atomic Physics, 16-21 July 2006, Innsbruck, Austria (Innsbruck University), p.238
- [10] R. W. P. Drever, J. L. Hall, F. V. Kowalski, J. Hough, G. M. Ford, A. J. Munley, and H. Ward, 1983, “*Laser phase and frequency stabilization using an optical-resonator*,” **Applied Physics**, **B31**, 97-105.
- [11] L. Ricci, M. Meidemuller, T. Esslinger, A. Hemmerich, C. Zimmermann, V. Vuletic, W. Kenig, and T. W. Hansch, 1995, “*A compact grating-stabilized diode-laser system for atomic physics*,” **Optical Communications**, **117**, 541-549.
- [12] D. M. Lucas, A. Ramos, J. P. Home, M. J. McDonnell, S. Nakayama, J.-P. Stacey, S. C. Webster, D. N. Stacey and A. M. Steane, 2004, “*Isotope-selective photoionization for calcium ion trapping*,” **Physical Review**, **A69**, 012711.
- [13] F. Torabi-Goudarzi and E. Riis, 2003, “*Efficient cw high-power frequency doubling in periodically poled KTP*,” **Optical Communications**, **227**, 389-403.
- [14] H. Sawamura, H. Kitamura, K. Toyoda, and S. Urabe, 2005, “*Observation of motional sidebands in single $^{40}Ca^+$ ions with improved detection efficiency*,” **Applied Physics** **B80**, 1011-1014.
- [15] D. Berkeland, J. D. Miller, J. C. Bergquist, W. M. Itano, and D. J. Wineland, 1998, “*Minimization of ion micromotion in a Paul trap*,” **Journal of Applied Physics**, **83**, 5025-5033.
- [16] T. Udem, R. Holzwarth, and T. W. Hansch, 2002, “*Optical frequency metrology*,” **Nature**, **416**, 233-237
- [17] H. Ito, S. Nagano, Y. Li, K. Matsubara, and M. Hosokawa, 2006, “*Development of optical frequency standards in NICT*,” in Proceedings of the 11th European Conference on Networks and Optical Communications, 12 July 2006, Berlin, Germany, p. 314.
- [18] L. Matos, D. Kleppner, O. Kuzucu, T. R. Schibli, J. Kim, E. P. Ippen, and F. X. Kaertner, 2004, **Optical Letters**, **29**, 1683-1685.

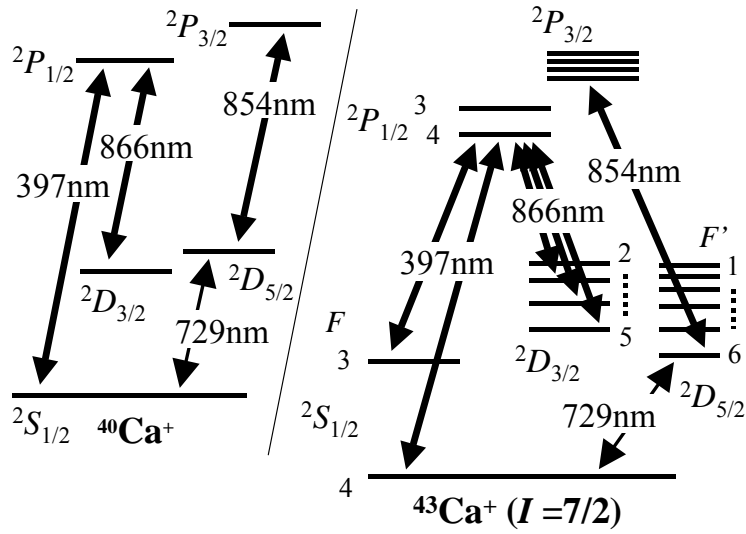


Figure 1. Partial term diagrams of $^{40}\text{Ca}^+$ and $^{43}\text{Ca}^+$. F and F' are total angular momentum, including nuclear spin $I=7/2$.

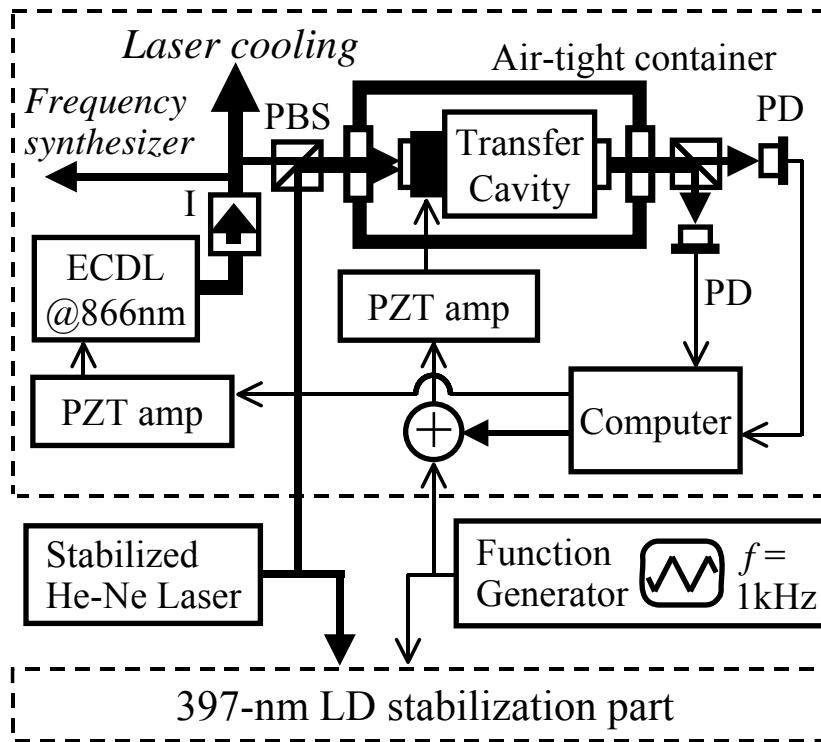


Figure 2. Light source system for laser cooling of $^{40}\text{Ca}^+$ ions. ECDL: extended cavity diode laser; I: isolator; PD: photodiode; PBS: polarized-beam splitter; PZT: piezo-transducer.

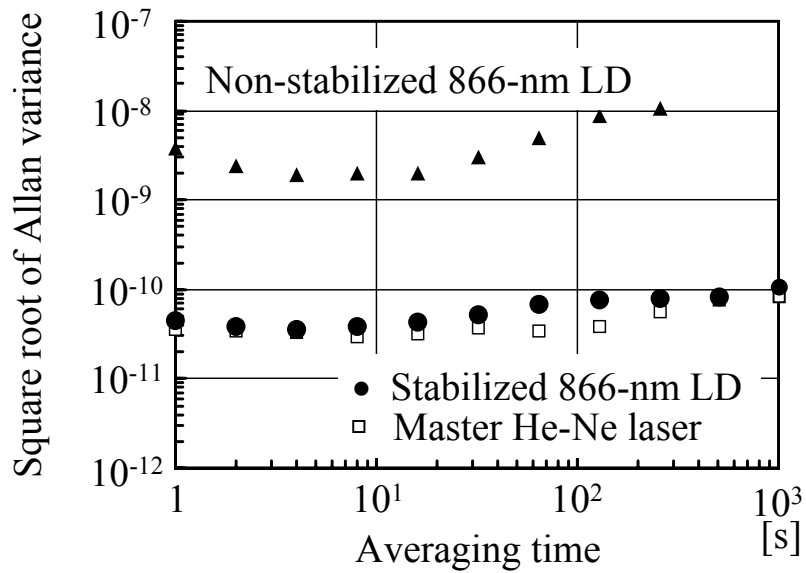


Figure 3. The Allan variance of (▲) the non-stabilized 866-nm ECDL, (●) the stabilized 866-nm ECDL, and (◻) the stabilized He-Ne laser.

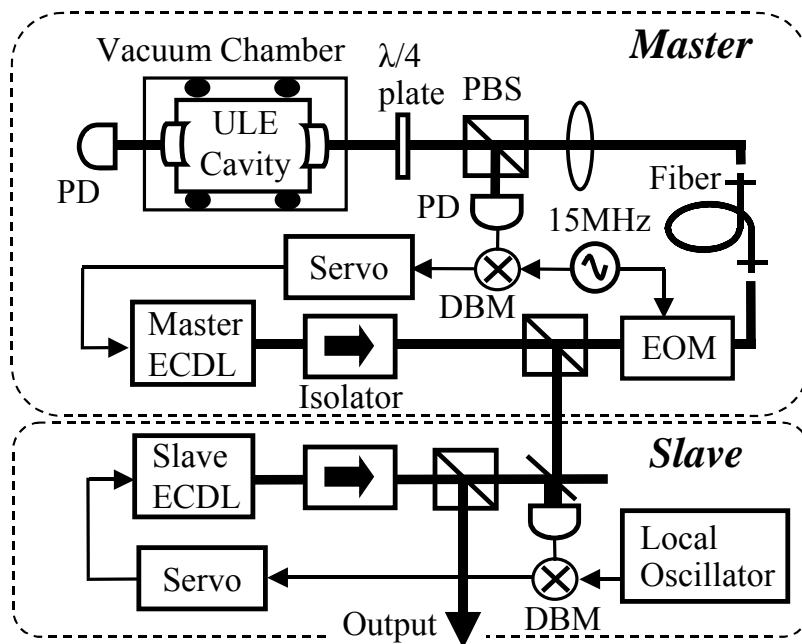


Figure 4. Light source for the quadrupole transition measurement. ULE cavity: ultra-low expansion optical cavity; DBM: double balanced mixer; EOM: electro-optic modulator.

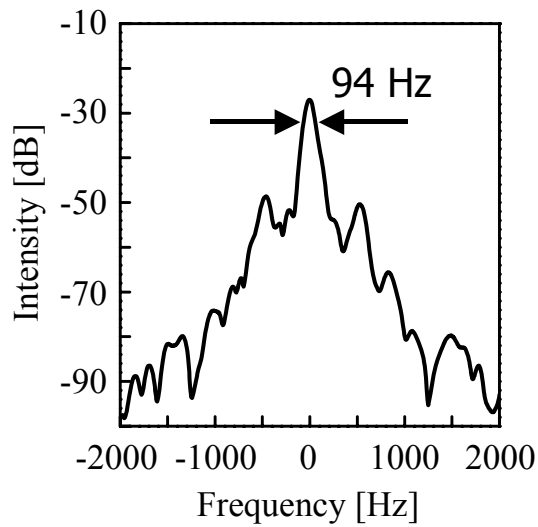


Figure 5. Spectrum of the beatnote between two laser beams stabilized to separate ULE resonant cavities. The linewidth of 66 Hz of each the clock laser is estimated from the linewidth at the -3 dB intensities from the maximum.

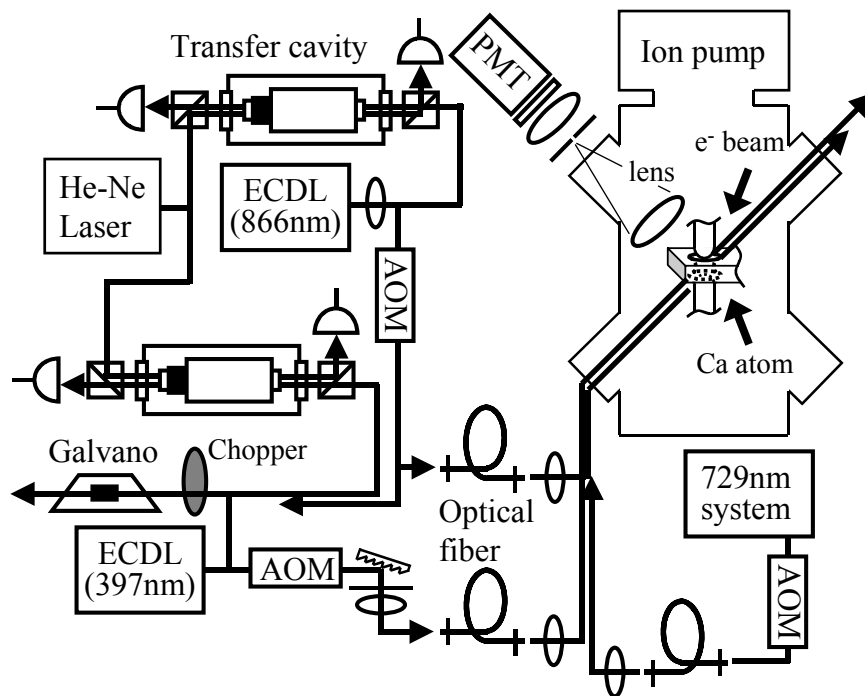


Figure 6. Experimental setup for single $^{40}\text{Ca}^+$ ions. AOM: acousto-optic modulator; PMT: photo-multiplier tube; Galvano: Galvano tube.

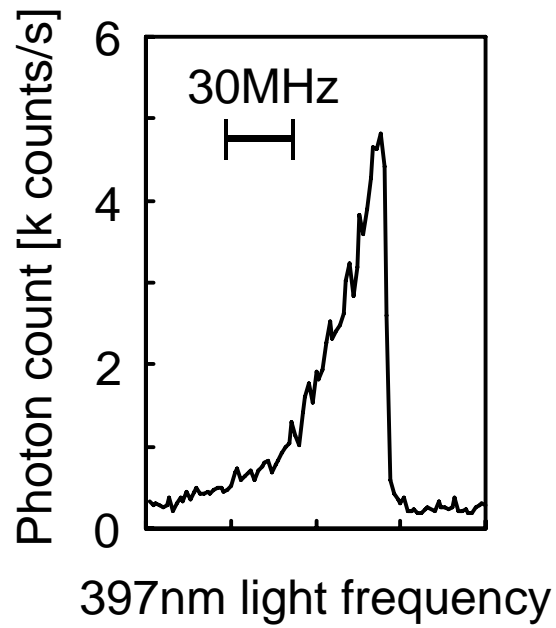


Figure 7. Spectrum of a laser-cooled single $^{40}\text{Ca}^+$ ion.

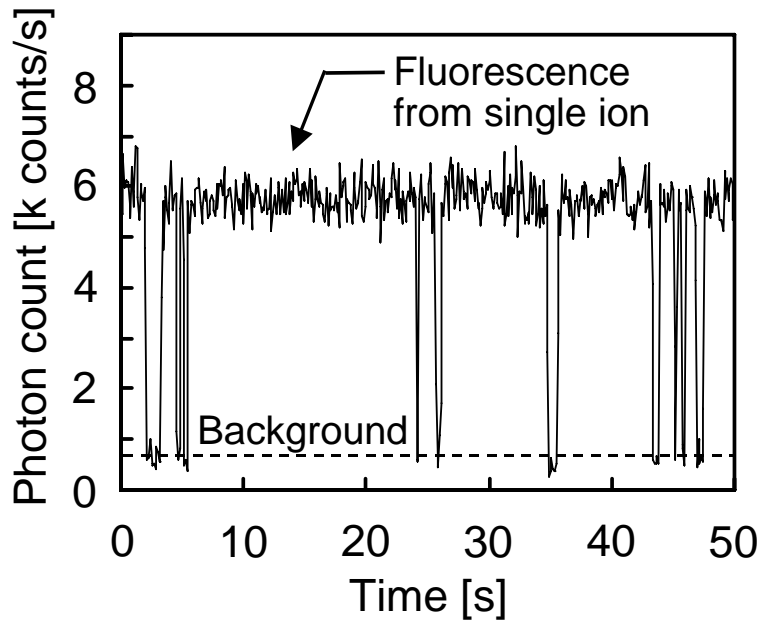


Figure 8. Quantum jumps of a single $^{40}\text{Ca}^+$ ion.

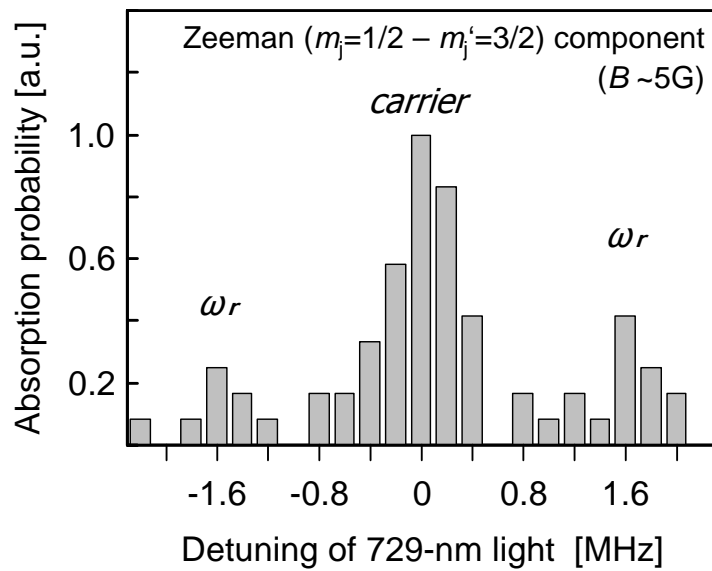


Figure 9. The $^2S_{1/2} - ^2D_{5/2}$ electric quadrupole transition. This is measured in an external magnetic field of ~ 5 G, and one Zeeman component is shown as a function of the 729-nm frequency detuning.

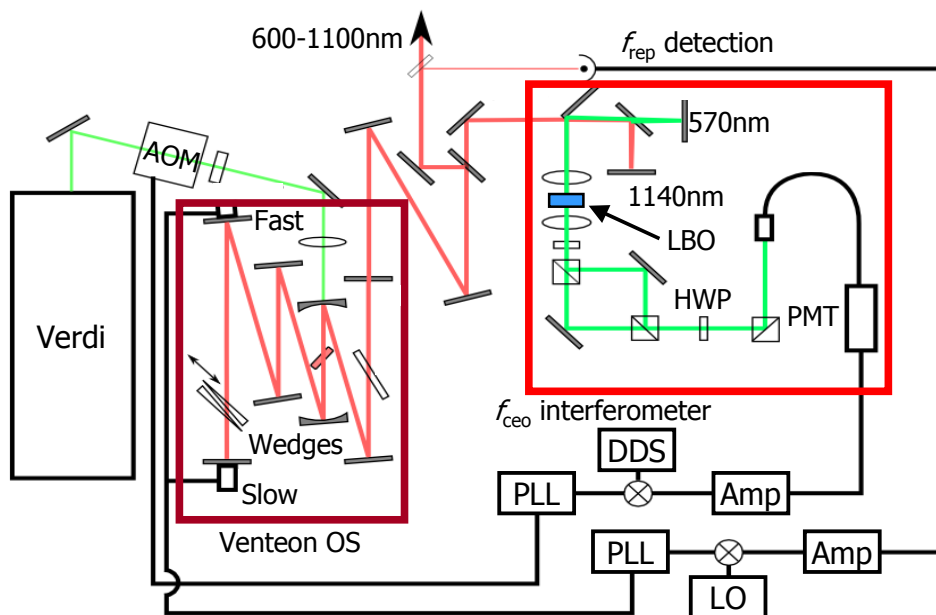


Figure 10. Experimental setup of the optical frequency comb using a VENTÉON OS.

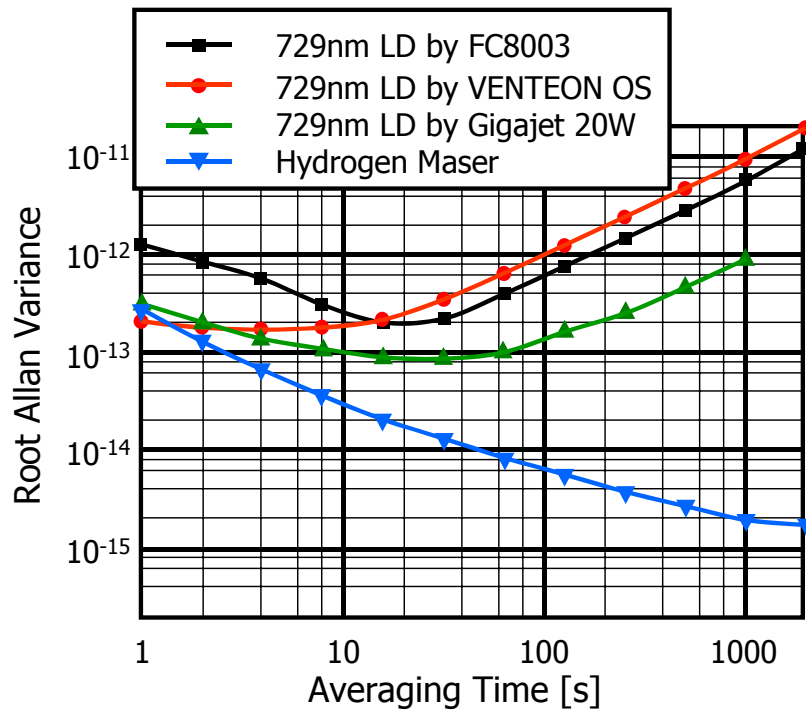


Figure 11. Frequency stability of the clock 729-nm laser measured by three optical frequency combs individually. A hydrogen maser is used as the frequency reference for the frequency combs.

